

The *n*-resolved single-electron capture in slow O^{6+}-Ne collisions

Shucheng Cui(崔述成), Dadi Xing(邢大地), Xiaolong Zhu(朱小龙), Maogen Su(苏茂根), Yong Gao(高永), Dalong Guo(郭大龙), Dongmei Zhao(赵冬梅), Shaofeng Zhang(张少锋), Yanbiao Fu(符彦飙), and Xinwen Ma(马新文)

Citation: Chin. Phys. B, 2024, 33 (**7**): 073401. DOI: 10.1088/1674-1056/ad39d2
Journal homepage: http://cpb.iphy.ac.cn; http://iopscience.iop.org/cpb

What follows is a list of articles you may be interested in

State-selective charge exchange cross sections in collisions of highly-charged sulfur ions with helium and molecular hydrogen

Xiaolong Zhu(朱小龙), Shucheng Cui(崔述成), Dadi Xing(邢大地), Jiawei Xu(徐佳伟), B. Najjari, Dongmei Zhao(赵冬梅), Dalong Guo(郭大龙), Yong Gao(高永), Ruitian Zhang(张瑞田), Maogen Su(苏茂根), Shaofeng Zhang(张少锋), and Xinwen Ma(马新文)

Chin. Phys. B, 2024, 33 (**2**): 023401. DOI: 10.1088/1674-1056/ad0b01

Electron excitation processes in low energy collisions of hydrogen-helium atoms

Kun Wang(王堃), Chuan Dong(董川), Yi-Zhi Qu(屈一至), Ling Liu(刘玲), Yong Wu(吴勇),Xu-Hai Hong(洪许海), and Robert J. Buenker

Chin. Phys. B, 2022, 31 (**12**): 123401. DOI: 10.1088/1674-1056/aca14c

Atomic structure and collision dynamics with highly charged ions

Xinwen Ma(马新文), Shaofeng Zhang(张少锋), Weiqiang Wen(汶伟强), Zhongkui Huang(黄忠魁), Zhimin Hu(胡智民), Dalong Guo(郭大龙), Junwen Gao(高俊文), Bennaceur Najjari, Shenyue Xu(许慎跃), Shuncheng Yan(闫顺成), Ke Yao(姚科), Ruitian Zhang(张瑞田), Yong Gao(高永), and Xiaolong Zhu(朱小龙)

Chin. Phys. B, 2022, 31 (**9**): 093401. DOI: 10.1088/1674-1056/ac8736

Charge transfer in low-energy collisions ofBe^{3+} and B^{4+} ions with He

Kun Wang(王堃), Yi-Zhi Qu(屈一至), Chun-Hua Liu(刘春华), Ling Liu(刘玲), Yong Wu(吴勇), H P Liebermann, Robert J. Buenker

Chin. Phys. B, 2020, 29 (**9**): 093401. DOI: 10.1088/1674-1056/aba276

Differential cross sections of positron—hydrogen collisions

Rong-Mei Yu(于荣梅), Chun-Ying Pu(濮春英), Xiao-Yu Huang(黄晓玉), Fu-Rong Yin(殷复荣), Xu-Yan Liu(刘旭焱), Li-Guang Jiao(焦利光), Ya-Jun Zhou(周雅君)

Chin. Phys. B, 2016, 25 (**7**): 073401. DOI: 10.1088/1674-1056/25/7/073401

DATA PAPER

The n-resolved single-electron capture in slow O^{6+}–Ne collisions

Shucheng Cui(崔述成)[1,2,†], Dadi Xing(邢大地)[1,2,†], Xiaolong Zhu(朱小龙)[2,3,‡], Maogen Su(苏茂根)[1], Yong Gao(高永)[2,3], Dalong Guo(郭大龙)[2,3], Dongmei Zhao(赵冬梅)[2,3], Shaofeng Zhang(张少锋)[2,3], Yanbiao Fu(符彦飙)[1,§], and Xinwen Ma(马新文)[2,3]

[1] *Key Laboratory of Atomic and Molecular Physics Functional Material of Gansu Province, College of Physics and Electronic Engineering, Northwest Normal University, Lanzhou* 730070, *China*

[2] *Institute of Modern Physics, Chinese Academy of Sciences, Lanzhou* 730000, *China*

[3] *University of Chinese Academy of Sciences, Beijing* 100049, *China*

(Received 7 February 2024; revised manuscript received 19 March 2024; accepted manuscript online 3 April 2024)

A study of single-electron capture (SEC) in 18–240 keV O^{6+}–Ne collisions has been conducted employing a combination of experimental and theoretical methodologies. Utilizing a reaction microscope, state-selective SEC cross sections and projectile scattering angle distributions were obtained. The translational energy spectra for SEC reveal the prevailing capture into $n = 3$ states of the projectile ion, with a minor contribution from $n = 4$ states. Notably, as the projectile's energy increases, the relative contribution of SEC $n = 4$ states increases while that of SEC $n = 3$ states diminishes. Furthermore, we computed state-selective relative cross sections and angular differential cross sections employing the classical molecular Coulomb over-the-barrier model (MCBM) and the multichannel Landau–Zener (MCLZ) model. A discernible discrepancy between the state-selective cross sections from the two theoretical models is apparent for the considered impact energies. However, regarding the angular differential cross sections, an overall agreement was attained between the current experimental results and the theoretical results from the MCLZ model.

Keywords: charge exchange, state-selective cross sections, angular differential cross sections, COLTRIMS

PACS: 34.70.+e, 95.30.Dr **DOI:** 10.1088/1674-1056/ad39d2

1. Introduction

The charge exchange (CX) phenomenon involving ions in highly charged states has not only significantly contributed to the comprehension of the fundamental quantum few-body problem within the Coulomb field but also finds practical applications in astrophysics, plasma studies, and the examination of biological radiation effects induced by charged ions.[1–5] The study of these phenomena greatly depends on precise collision cross sections, which are crucial for acquiring foundational insights into reaction dynamics that are essential for understanding complex systems. CX, where electrons are transferred from a neutral atomic or molecular target to ions in highly charged states, has garnered significant attention following the initial ROSAT telescope's 1996 B2 comet Hyakutake x-ray images.[1] Highly charged ions, such as (O^{6+}, C^{5+}, N^{6+}, and Ne^{8+}), represent a small fraction of solar wind ions, but contribute significantly to x-ray emissions from various astrophysical and environmental sources.[6–8] The single electron capture (SEC) process is the dominant reaction in the CX between solar wind ions and planetary, cometary atmospheres and interstellar neutrals, and the subsequent x-rays emitted by the de-excitation of excited highly charged ions, which is an important source of soft x-rays in interstellar space. CX measurements provide a new approach to study soft x-ray background radiation in interstellar environments. To understand the observed x-ray spectra, more atomic data on CX is needed. Two classical models are commonly used to describe the characterization of captured electronic states in ion–atom collisions involving electron capture. The frequently used molecular Coulomb over-the-barrier model (MCBM)[9] predicts state distributions and state-selective cross sections of ion-captured electrons via a calculated reaction window, typically represented as a Gaussian distribution of absolute cross sections for specific capture processes related to energy loss Q. The alternative multichannel Landau–Zener (MCLZ) model[10–12] suggests that electron transfer predominantly occurs at the intersection of the incident and exit channels, albeit with limited accuracy, offering a better description of angular differential cross sections in the capture process.

Over the past two decades, there has been continuous interest in studying the collision dynamics between solar wind ions and neutral atoms or molecules. Nevertheless, investigations concerning charge exchange processes involving O^{6+} ions remain relatively scarce. On the theoretical front, Fritsch *et al.* developed the atomic orbital expansion-based close-coupling method (AOCC) and presented calculated cross sections for one-electron transfer in O^{6+}–He collisions in the energy range of 0.5–40 keV/u.[13] Furthermore, Zhao *et al.*

[†]The first two authors contributed equally to this paper.

[‡]Corresponding author. E-mail: zhuxiaolong@impcas.ac.cn

[§]Corresponding author. E-mail: fuyb@nwnu.edu.cn

© 2024 Chinese Physical Society and IOP Publishing Ltd

employed a two-center atomic orbital close-coupling method (TC-AOCC) to explore the electron capture process in O^{6+} collisions with He and H_2 ground states, providing total and state-selective electron capture cross sections for collision energies between 0.5 keV/u and 300 keV/u.[14] Additionally, methodologies such as molecular orbital expansion and classical trajectory Monte Carlo (CTMC) have been utilized to study the O^{6+}–He collision system.[15,16]

Regarding experimental studies, the focus has primarily been on total cross sections and state-selective cross sections with He and H_2 targets. In the collision energy range from 19.5 keV/u to 100 keV/u, Cao *et al*. systematically measured state-resolved SEC between O^{6+} ions and He/H_2.[17] Similarly, Kitazawa *et al*. explored electron energy spectra resulting from collisions between O^{6+} ions and rare gas atoms (He, Ne, and Ar) using zero-degree Auger electron spectroscopy with high energy resolution.[18] However, research on the SEC process between O^{6+} ions and Ne targets remains unexplored, both theoretically and experimentally.

To precisely determine the velocity, species, and abundance of solar wind ions, it is crucial to carry out experimental studies on the collision system of O^{6+}–Ne. To address this research gap, in the present study we systematically measured the recoil ion momentum of SEC in collisions of O^{6+} ions with Ne at impact energies ranging from 18 keV to 240 keV. The experiments were conducted on the Electron Beam Ion Source (EBIS) platform in conjunction with cold target recoil ion momentum spectroscopy (COLTRIMS).[19,20] The principal quantum number-resolved state-selective, partial cross sections, and angular distributions of the projectile ions in the single electron capture process were obtained.

2. Experimental setup

This experiment was conducted on the EBIS platform of the Institute of Modern Physics, Chinese Academy of Sciences. The experimental setup is depicted in Fig. 1. Detailed procedures have been previously documented,[17,19,20] and only a succinct overview is provided here. Oxygen is introduced into the EBIS to generate oxygen ions with varying charge states. These ions are then extracted and sorted by a charge state analyzer to isolate the O^{6+} ion beam that is essential for the experiment. Subsequently, the ions are adjusted to the requisite energy for the experiment, passing through a two-dimensional beam-limiting diaphragm and entering a target chamber to collide perpendicularly with the supersonic Ne target located at the central axis of the time-of-flight (TOF) spectrometer. Recoil target ions produced from these collisions are extracted by a uniform electric field ($E_{\mathrm{TOF}} \approx 3$ V/cm) oriented perpendicular to both the beam and target directions. They are then detected by a two-dimensional, position-sensitive microchannel plate detector. Post-reaction, scattered projectile ions with various charge states are analyzed by an electrostatic analyzer downstream of the reaction point. Projectiles with reduced charge states are identified by another position-sensitive detector positioned behind the beam, while unreacted projectiles are collected by the Faraday cup. The TOF spectrometer comprises an acceleration region and a drift region, which is used to measure the TOF of recoil ions. The experiment utilizes a dual coincidence measurement technique between scattered ions and recoil ions, coupled with an event recording mode measurement. Through analysis of the two-dimensional correlation spectrum between ion positions on the scattering detector and the TOF of the recoil ions, identification of reaction channels such as SEC and multiple-electron capture becomes feasible. For specific reaction channels, analyzing the recoil ion positions on the recoil detector and measuring their time of flight enables the reconstruction of the three-dimensional momentum of the recoil ions.

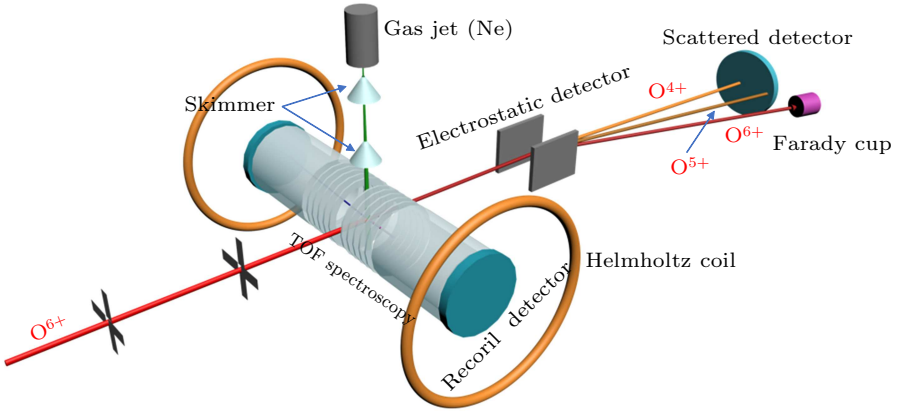


Fig. 1. The experimental scheme of COLTRIMS.

In Fig. 1, the momentum measured along the beam's current direction defines the longitudinal momentum of the recoil ion (P_{long}), while the momentum perpendicular to the beam's direction defines the transverse momentum of the recoil ion (P_{trans}). The fundamental principle of COLTRIMS relies on establishing a relationship between the recoil-ion momentum

and two crucial parameters: the Q value representing the binding energy change before and after the collision, and the scattering angle θ of the projectile ion.[21,22] This capture process can be conceptually viewed as an inelastic two-body collision in terms of kinetics. Hence, adhering to the conservation laws of energy and momentum, a simple relation can be derived for small scattering angles:

$$Q = -v_{\rm o} \cdot P_{\rm long} - \frac{n}{2} \cdot v_{\rm o}^2, \tag{1}$$

$$\theta = \frac{P_{\rm trans}}{P_{\rm o}}. \tag{2}$$

Here, Q encapsulates details regarding the alteration in binding energy, offering insights into the state populated on the projectile due to the capture process. The variables $v_{\rm o}$, n, $P_{\rm o}$, and θ denote the projectile's velocity, the number of electrons captured by the projectile, the initial momentum of the projectile ion, and the scattering angle of the projectile ion, respectively. It is important to note that all quantities in the equations above are presented in atomic units.

3. Results and discussion

We present the results concerning the relative n-state-selective cross sections for SEC in O^{6+} collisions with neon. The $P_{\rm long}$ distributions have been converted into Q-value distributions using Eq. (1). Figure 2 illustrates the measured Q spectra of SEC in O^{6+}–Ne collisions at impact energies ranging from 18 keV to 240 keV. The experimental results demonstrate that the SEC to the $n = 3$ states of the projectile ion is the most significant capture channel, while the capture to the $n = 4$ states stands as the second important capture channel, and its importance increases with the increase in the energy of the projectile. Our current measurements exhibit that with the escalation in collision energy, the population ratio of the $n = 4$ state also increases. In other words, as the projectile's energy rises, the captured state tends towards a higher quantum state. This observed trend is consistent with the conclusions given by Abdallah *et al.*[23]

Moreover, figure 2 presents the reaction window calculated by the MCBM, with its peak value normalized to the peak value of the experimental measurement for comparative analysis. The predicted reaction window by the theory essentially encompasses the primary reaction channels observed in the experimental results. The position of the red vertical lines is in response to the Q-values of the final channel, and the height of the red line reflects the relative state-selective population of different reaction channels. This characteristic helps to determine the state resolution cross sections of SEC to different principal quantum numbers n, as calculated by the MCBM. In contrast to the experimental results, the relative cross sections predicted by MCBM at the energy of 240 keV agree very well with the experimental results, whereas the relative cross sections at all other energies do not.[24]

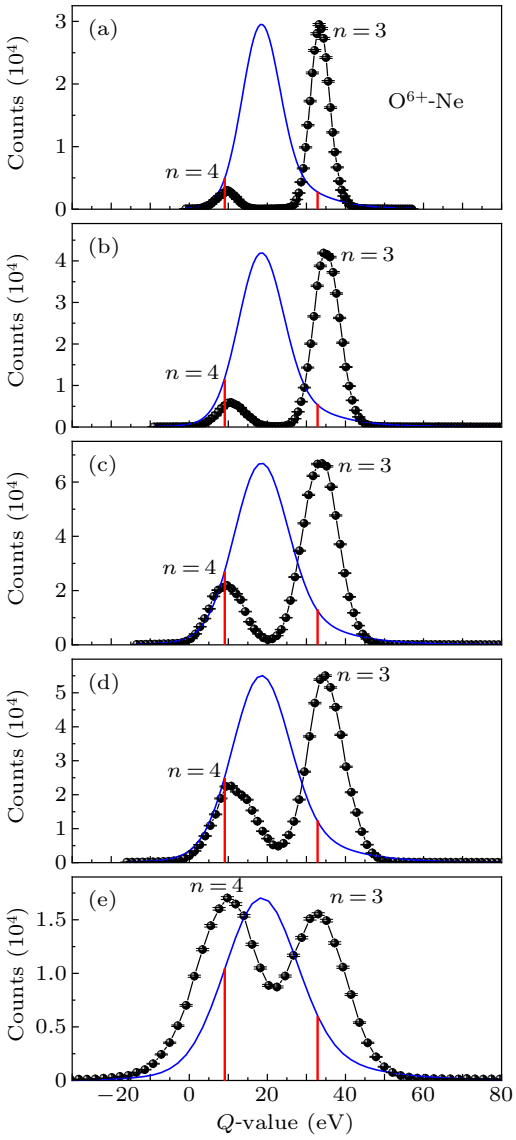


Fig. 2. Measured Q spectrum of SEC between O^{6+} and Ne with different incident projectile energies: (a) 18 keV, (b) 36 keV, (c) 72 keV, (d) 96 keV, (e) 240 keV. The black solid circles and the black solid line are the results of the experimental measurement, and the blue solid line is the reaction window calculated by MCBM normalized to the peak heights of the experimental measurement. The thick red vertical lines represent the intensity of state-selective cross sections for MCBM calculations.

To quantitatively illustrate the correlation between the relative state-selective cross sections of SEC and collision energy, and to compare the disparities between experimental and theoretical results, figure 3 presents the O^{6+}–Ne SEC state-selective cross sections. This is juxtaposed against the results computed by MCLZ and MCBM. In Fig. 3, solid symbols connected with solid lines represent experimental measurements, while open symbols connected with solid lines depict MCBM calculations, and open symbols connected with dashed lines reflect MCLZ calculations. Different capture channels are denoted by distinct colors and symbols. Analysis of Fig. 3 reveals that the relative cross sections of the primary capture

state ($n = 3$) observed in the experiment diminish with escalating collision energy. Conversely, the cross sections of the secondary reaction channel ($n = 4$) increase with the increase in collision energy. The results derived from both MCLZ and MCBM theoretical calculations exhibit inadequacies.

Unfortunately, it seems that MCBM is not appropriate for the O^{6+}–Ne collision system. This method relies solely on the binding energy of active electrons before and after collisions, as well as collision velocity. As for the MCLZ model, based on the fact that the coupling matrix elements are much smaller for multi-electron exchange processes than for single-electron exchange, after several trials it was found that the results calculated by MCLZ with the coupling matrix elements, reduced by 20% from Olson and Salop's results, show a good agreement with our experimental results of the lowest impact energy.[25,26] However, the agreement between MCLZ and the experimental results is reasonable only at lower collision energies. As collision energy increases, the $n = 3$ reaction channel is significantly overestimated, while the $n = 4$ channel is notably underestimated. The discrepancies between theoretical predictions and experimental measurements are inferred from the fact that the two classical models entirely disregard electron–electron correlations during the calculation.[24,25] This may indicate that electron–electron correlations play an important role during SEC. In addition, there are discrepancies between two theoretical predictions. This may happen because the MCBM utilizes a hydrogen-ion-like (static) model to calculate the capture probability and the MCLZ model calculates the transition (capture) probability by solving the Schrödinger equation, even though the interaction matrix elements mentioned therein are given according to the empirical formulas mentioned earlier.[25]

The scattering angle distributions depicting the SEC process in O^{6+}–Ne collisions across various collision energies are presented in Fig. 4. Examination of the figure reveals that the scattering angle distribution shifts towards smaller angles with increasing collision energy. Notably, there is an absence of distinct oscillatory structure in both the total angular distribution and the distribution pertaining to individual capture channels. Additionally, the average scattering angle demonstrates a shift towards larger values with a decreasing principal quantum number n.

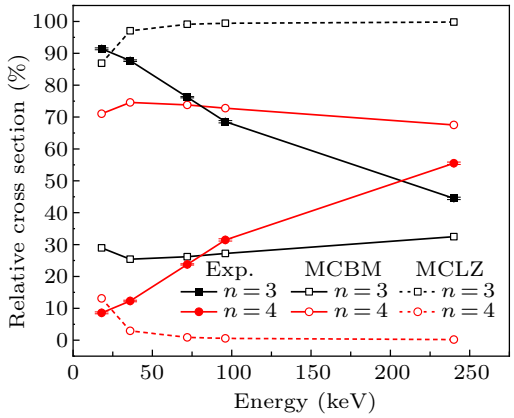


Fig. 3. O^{6+}–Ne SEC relative state-selective cross sections, the solid shape and the solid line are the result of experimental measurement, the open shape and solid line are the result of MCBM calculation, the open shape and the dashed line is the result of MCLZ calculation, and different colors and symbols represent different capture channels.

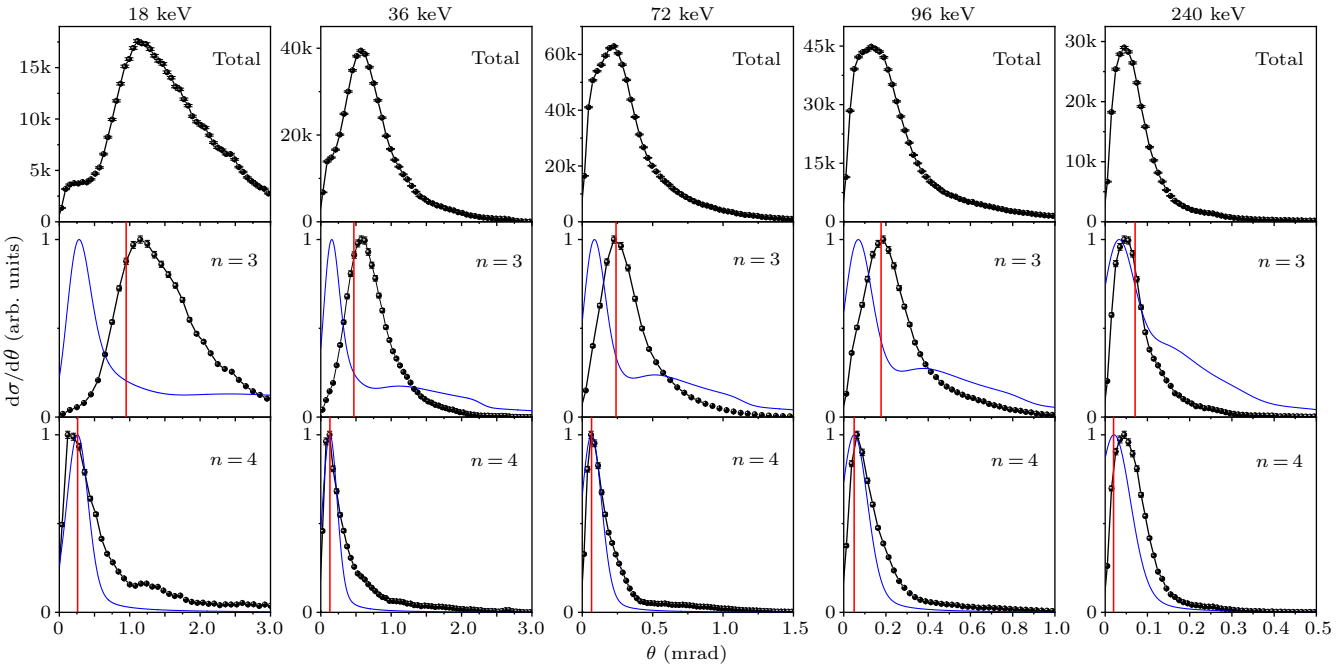


Fig. 4. Total scattering angle distributions of the SEC in O^{6+}–Ne collisions at different collision energies and scattering angle distributions into $n = 3$ and $n = 4$ states. The vertical lines locate the half-Coulomb scattering angles. The blue solid lines represent the calculations of an MCLZ model by using the method of Andersson *et al.*[10,12] Both experimental and model curves have been normalized to a peak value of unity.

In Fig. 4, the red vertical line signifies the half-Coulomb angle, $\theta_c = Q/(2E)$ (E is the projectile energy), which is related to an impact parameter equal to the crossing radius in the curve-crossing picture if Coulomb potential curves are involved. As discussed in previous studies,[10,23,27,28] when traversing an entrance channel or exit channel within a curve-crossing space along a semi-classical trajectory, deflections occur with angles larger (or smaller) than θ_c. Notably, the scattering angle for capture into $n = 3$ and $n = 4$ states appears to peak around θ_c. For a quantitative analysis of the data, calculations were conducted for the O^{6+}–Ne collision system utilizing the method proposed by Anderson *et al.*[10,12] Both experimental and theoretical values were normalized to a peak value of unity. The predictions for capture into $n = 4$ states are more accurate than those for $n = 3$ states. Similar results are also observed in Ar^{16+}–He/Ne and Ar^{18+}–He collisions.[23,28,29] In addition, the predictions for capture into $n = 3$ states become better as impact energy increases. We infer that this discrepancy stems from the fact that only the local interaction near the crossing is considered in the MCLZ model. For a better description of the present experimental results, new theoretical work is needed.

4. Conclusions

We measured the n-resolved SEC process in slow O^{6+}–Ne collisions at energies ranging from 18 keV to 240 keV by COLTRIMS. The Q-value and scattering angle distributions were obtained. The observed Q-value spectrum of single-electron capture shows that at low energies the dominant reaction channel is single-electron capture into the $n = 3$ states, whereas at 240 keV single-electron capture into the $n = 4$ states becomes the dominant reaction channel. These results agree with those of the MCLZ calculation at the collision energy of 18 keV. Regarding the experimentally measured angular distribution of the projectile, it shows a shift towards smaller angles with the increase in the collision energy. Specifically, the scattering angle distribution of a single electron captured into the principal quantum number $n = 4$ states at small angles, whereas the distribution for capture into $n = 3$ states at larger scattering angles. This observation coincides with the results of the MCLZ calculations.

Data availability statement

The data that support the findings of this study are openly available in Science Data Bank at https://doi.org/10.57760/sciencedb.15984.

Acknowledgements

Project supported by the National Natural Science Foundation of China (Grant Nos. 11934004, 12064040, and 11974358), the National Key Research and Development Program of China (Grant No. 2022YFA1602500), and Strategic Key Research Program of the Chinese Academy of Sciences (Grant No. XDB34020000). We thank the fruitful discussion with Dr. B. Najjari. The authors thank the staff of 320 kV and EBIS platforms for their technical support.

References

[1] Lisse C, Dennerl K, Englhauser J, Harden M, Marshall F, Mumma M, Petre R, Pye J, Ricketts M, Schmitt J, *et al*. 1996 *Science* **274** 205
[2] Haberli R M, Gombosi T I, De Zeeuw D L, Combi M R and Powell K G 1997 *Science* **276** 939
[3] Janev R K, Presnyakov L P and Shevelko V P 2012 *Physics of highly charged ions* Vol. 13 (Springer Science & Business Media)
[4] Isler R 1994 *Plasma Physics and Controlled Fusion* **36** 171
[5] Cravens T 1997 *Geophysical Research Letters* **24** 105
[6] Chuanxi X, Jiawei X, Xiaolong Z, Maogen S, Dongmei Z, Daolong G, Yong G, Zhang R, Shuncheng Y, Zhang S, *et al*. 2021 *Nuclear Physics Review* **38** 452
[7] Fischer D, Feuerstein B, Dubois R D, Moshammer R, López-Urrutia J C, Draganic I, Lörch H, Perumal A N and Ullrich J 2002 *J. Phys. B: Atom. Mol. Opt. Phys.* **35** 1369
[8] Roncin P, Barat M and Laurent H 1986 *Europhys. Lett.* **2** 371
[9] Niehaus A 1986 *J. Phys. B: Atom. Mol. Phys.* **19** 2925
[10] Andersson L, Danared H and Barany A 1987 *Nucl. Instr. Meth. B* **23** 54
[11] Olson R and Salop A 1977 *Phys. Rev. A* **16** 531
[12] Andersson L, Pedersen J, Barany A, Bangsgaard J and Hvelplund P 1989 *J. Phys. B: Atom. Mol. Opt. Phys.* **22** 1603
[13] Fritsch W and Lin C 1986 *J. Phys. B: Atom. Mol. Phys.* **19** 2683
[14] Zhao Y, Liu L, Xue P, Wang J and Janev R 2010 *J. Phys. B: Atom. Mol. Opt. Phys.* **43** 185202
[15] Shimakura N, Sato H, Kimura M and Watanabe T 1987 *J. Phys. B: Atom. Mol. Phys.* **20** 1801
[16] Machacek J, Mahapatra D, Schultz D, Ralchenko Y, Chutjian A, Simcic J and Mawhorter R 2014 *Phys. Rev. A* **90** 052708
[17] Cao T, Meng T, Gao Y, Zhang S, Zhang R, Yan S, Zhu X, Wang J, Ma P, Ren B, *et al*. 2023 *The Astrophysical Journal Supplement Series* **266** 20
[18] Kitazawa S, Iemura K, Ohtani S, Koide M, Suzuki H, Sekiguchi M, Takayanagi T, Machida S and Wakiya K 1997 *Physica Scripta* **1997** 207
[19] Ma X, Zhang R, Zhang S, Zhu X, Feng W, Guo D, Li B, Liu H, Li C, Wang J, *et al*. 2011 *Phys. Rev. A* **83** 052707
[20] Zhu X, Ma X, Li J, Schmidt M, Feng W, Peng H, Xu J, Zschornack G, Liu H, Zhang T, *et al*. 2019 *Nucl. Instr. Meth. B* **460** 224
[21] Ullrich J, Moshammer R, Dörner R, Jagutzki O, Mergel V, Schmidt-Böcking H and Spielberger L 1997 *J. Phys. B: Atom. Mol. Opt. Phys.* **30** 2917
[22] Dörner R, Mergel V, Jagutzki O, Spielberger L, Ullrich J, Moshammer R and Schmidt-Böcking H 2000 *Physics Reports* **330** 95
[23] Abdallah M, Wolff W, Wolf H, Kamber E, Stöckli M and Cocke C 1998 *Phys. Rev. A* **58** 2911
[24] Chen L F, Ma X W and Zhu X L 2006 *Acta Phys. Sin.* **55** 6347 (in Chinese)
[25] Olson R and Salop A 1976 *Phys. Rev. A* **14** 579
[26] Kimura M, Iwai T, Kaneko Y, Kobayashi N, Matsumoto A, Ohtani S, Okuno K, Takagi S, Tawara H and Tsurubuchi S 1984 *J. Phys. Soc. Jpn.* **53** 2224
[27] Tunnell L, Cocke C, Giese J, Kamber E, Varghese S and Waggoner W 1987 *Phys. Rev. A* **35** 3299
[28] Xue Y, Ginzel R, Krauß A, Bernitt S, Schöffler M, Kühnel K, López-Urrutia J C, Moshammer R, Cai X, Ullrich J, *et al*. 2014 *Phys. Rev. A* **90** 052720
[29] Cassimi A, Duponchel S, Flechard X, Jardin P, Sortais P, Hennecart D and Olson R 1996 *Phys. Rev. Lett.* **76** 3679